PERFORMANCE ANALYSIS OF A REVOLVING VANE EXPANDER IN AN ORGANIC RANKINE CYCLE WITH HYDROFLUOROOLEFINS (HFOS) IN PLACE OF R134A

Ali Naseri*, Stuart Norris, Alison Subiantoro

Department of Mechanical Engineering,
Faculty of Engineering,
The University of Auckland,
Auckland, New Zealand
anas222@aucklanduni.ac.nz

* Corresponding Author

ABSTRACT

The Organic Rankine Cycle (ORC) is a promising method to exploit low to medium temperature heat sources. Though it is a mature technology, the selection, sizing and optimisation of the expander used to extract energy is still an active topic of research since it can strongly affect the performance of the ORC. Among the types of volumetric expanders, the use of rotary vane expanders is advantageous, particularly in small-scale applications, due to their simplicity, low manufacturing and maintenance cost, low noise, and high volumetric expansion ratios. However, they generally perform poorly in comparison to other rotary machines because of their inevitable leakage and friction losses, leading to low efficiencies. A Revolving Vane (RV) expander, in which both the rotor and cylinder rotate, unlike conventional vane-type mechanisms, has been shown to exhibit a significant reduction in friction losses. Such a machine has been previously studied in compressed air and refrigeration systems, but not in an ORC system.

In this study, the first law of thermodynamics is used to evaluate the performance of a Revolving Vane expander within an ORC system using R134a, R1234yf and R1234ze(E). The last two fluids are popular replacements for R134a, since they have low global warming and zero ozone depletion potentials. Previously developed mathematical models of the RV expander have been adopted for the study. Various operating conditions are simulated to find the optimal performance parameters of the expander using the chosen working fluids. The results demonstrate the potential of the RV expander for small-scale ORC applications. Moreover, the characteristics of the expander at various operating conditions are observed, showing that the expander design is suitable for small-scale ORC applications.

1. INTRODUCTION

Organic Rankine Cycles (ORCs) are a promising method to exploit various ranges of heat sources from low to medium temperatures and produce mechanical energy with the potential of integration into distributed power generation systems. An ORC comprises an evaporator, a condenser, a pump and an expansion machine as the four main components like a conventional steam cycle, but uses a low-boiling temperature organic substance as the working fluid (Bao and Zhao, 2013). However, adverse environmental effects of some of these working fluids has been of concern. This has initiated the phasing out of contributing fluids to ozone depletion and global warming such as Chlorofluorocarbons (CFCs) and Hydrochlorofluorocarbons (HCFCs) (Molés *et al.*, 2017). Although Hydrofluorocarbons (HFCs) are already dominating the refrigerant market because of their promising features especially in ORCs, their use will be phased out due to their high global warming potential. Meanwhile, Hydrofluoroolefins (HFOs) have drawn attention as a drop-in replacement for some conventional working fluids due to their environment friendly characteristics (Giuffrida, 2018).

Though ORC is a mature technology, the selection, sizing and optimisation of the expander used to extract energy is still an active topic of research since it can strongly affect the performance of the ORC. The expanders for ORC are classified into volume and velocity types. In a volumetric type expander, alteration of chambers' volume within the expander causes a decrease in working fluid pressure leading to the fluid expansion. This alteration is because of the relative position of the parts that defines a series of working chambers. Such expanders are the dominant type in small-scale power production. In a velocity type expander the created dynamic head of continuous flow of working fluid through the expander leads to work extraction within the expander (Badr *et al.*, 1984; Lemort and Legros, 2017). Among the available volumetric expanders, rotary vane expanders are attractive due to their simplicity, low manufacturing and maintenance cost, low noise, and high volumetric expansion ratios (Lemort *et al.*, 2009; Imran *et al.*, 2016). However, they generally perform poorly in comparison to other rotary machines because of the inevitable leakage and friction losses, leading to low efficiencies. The Revolving Vane (RV) mechanism was introduced to overcome these limitations (Ooi and Teh, 2012). Previous studies have demonstrated a potentially significant reduction in friction losses in compressed air and refrigeration systems (Subiantoro and Ooi, 2014). This concept comprises an eccentric rotor and cylinder that rotate synchronously with respect to their relative axis of rotations as illustrated in Figure 1, unlike conventional vane-type mechanisms. By fixing the vane onto the rotor, the vane side friction is significantly reduced; and since no contact occurs when the vane moves in its slot on the cylinder, the vane tip friction is eliminated. Moreover, the reduced relative velocity between the rotor and the cylinder alleviates the end face friction (Subiantoro and Tiow, 2009).

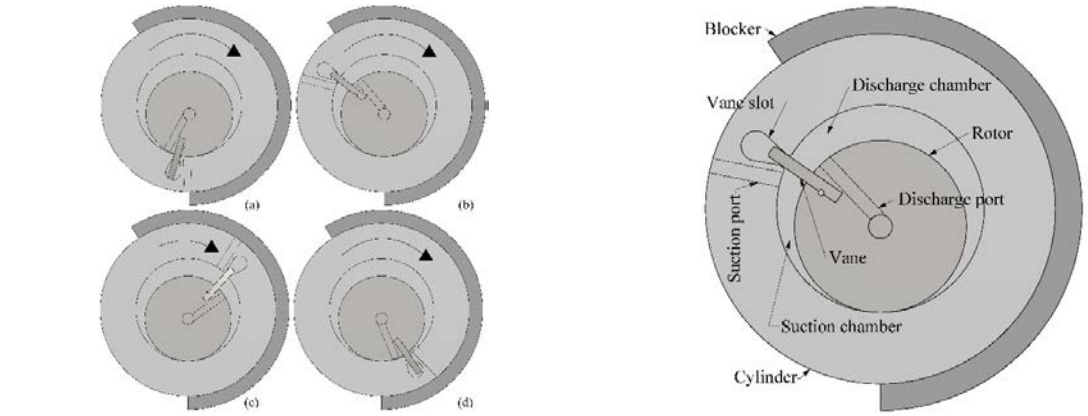

Figure 1: Revolving Vane Expander (A) mechanism (B) detailed schematic.

2. MATERIALS AND METHODS

2.1 Organic Rankine Cycle modelling

Figure 2(A) shows a basic ORC simulation model. The working fluid is pressurized using a pump to a higher pressure before entering the evaporator. It is heated in the evaporator to a specific temperature and then passes through the expander. The low-pressure working fluid is then condensed in the condenser after leaving the expansion machine. Both HFO-1234yf and HFO-1234ze(E) have negligible Ozone Depletion Potential (ODP) and Global Warming Potential (GWP) (Yamada *et al.*, 2012). It is worth to mention that these HFOs have similar thermodynamic properties to R134a and they are isentropic fluids, meaning that the slope of saturation vapour line is almost infinite. Hence, there is no need for superheating, since it has negligible effect on the thermal efficiency of the cycle (Dai *et al.*, 2009). Figure 2(B) shows the *T-s* diagram for ORC with R1234yf, assuming isentropic expansion and compression. Applying the principle of conservation of mass and energy to each component within the cycle, the general equations for the ORC can be expressed using Equations (1) to (6). It is noteworthy

that ε_{exp} is the "internal isentropic effectiveness" of the expander that is calculated from the power output from the expander over power that would be produced if the fluid undergoes an isentropic expansion through the expander (Lemort and Legros, 2017). It is assumed that heat is perfectly transferred within the heat exchangers with no sub-cooling and superheating, and the pumping process is isentropic.

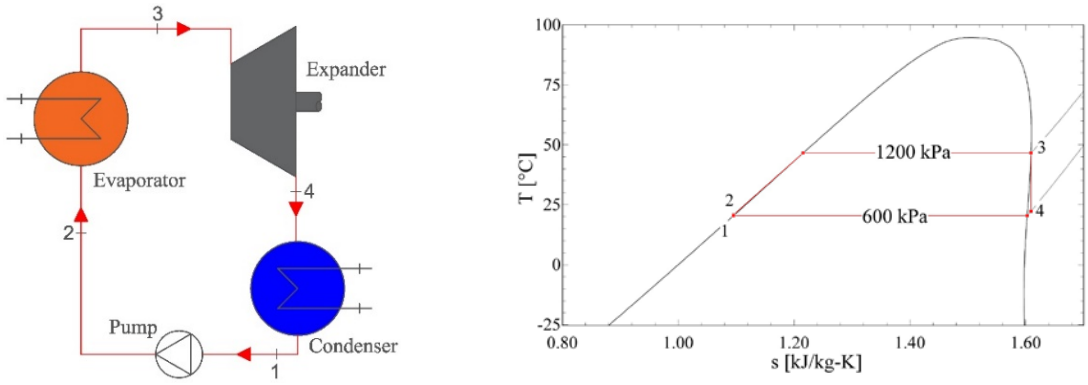

(A) (B)

Figure 2: (A) Rankine cycle schematic, (B) *T-s* diagram for ORC with R1234yf as its working fluid.

$$Q_{evaporator} = \dot{m}\left(h_3 - h_2\right) \tag{1}$$

$$Q_{condenser} = \dot{m}\left(h_4 - h_1\right) \tag{2}$$

$$W_{pump} = \dot{m}\left(h_1 - h_2^a\right) \tag{3}$$

$$\eta_{cycle} = \left(P - \dot{m}\left(h_1 - h_2^a\right)\right) \Big/ \left(\dot{m}\left(h_3 - h_2^a\right)\right) \tag{4}$$

$$W_{\exp ander}^{is} = \dot{m}\left(h_3 - h_4^{is}\right) \tag{5}$$

$$\varepsilon_{\exp ander} = P \Big/ \left(\dot{m}\left(h_3 - h_4^{is}\right)\right) \tag{6}$$

2.2 Revolving Vane Expander modelling

In this study, it is assumed the expander is adiabatic and the valve responses instantaneously at the desired moments of opening and closure. The expander is modelled using the operational and dimensional conditions tabulated in Table 1. These conditions are based on the actual Revolving Vane expander prototype, which was recently manufactured at the University of Auckland. The expander model comprises dynamics, thermodynamics and dynamics parts as follows. The interested reader is referred to (Subiantoro, 2012) for detailed equations.

Table 1: Operational and dimensional conditions.

Operation/dimension	**Value**	**Operation/dimension**	**Value**
Expander rotational speed (*rpm*)	1000	Rotor rotating inertia ($kg.mm^2$)	241
Rotor radius (*mm*)	29	Cylinder rotating inertia ($kg.mm^2$)	3239
Cylinder radius (*mm*)	35	Suction port area (mm^2)	96.36
Vane length (*mm*)	16	Discharge port area (mm^2)	49.85
Vane width (*mm*)	4	Ports coefficient of discharge	0.7
Expander length (*mm*)	29	Eccentricity (*mm*)	6
Suction pressure (*bar*)	12.0	Expander swept volume (cm^3)	32
Discharge pressure (*bar*)	6.0	Volumetric efficiency (%)	40

Figure 3 illustrates a free body diagram for the expander. The length of the exposed vane (l_{ve}) and the vane velocity are obtained using Equations (7) and (8) (Subiantoro and Tiow, 2009).

$$l_{ve} = -e\cos\varphi_r - r_r + \sqrt{r_c^2 - e^2\sin^2\varphi_r} \tag{7}$$

$$\frac{dl_{ve}}{dt} = \omega_r e\sin\varphi_r\left(1 - \frac{e\cos\varphi_r}{\sqrt{r_c^2 - e^2\sin^2\varphi_r}}\right) \tag{8}$$

To calculate the working chambers volume, Equation (9) is used (Subiantoro and Tiow, 2009).

$$V_{working\ chamber} = l_{expander}\int_0^{4\pi} l_{ve}\,d\varphi_r \tag{9}$$

In order to model the working chambers in an RV expander, the chambers are modelled as control volumes and the conservation of mass and energy is applied, which can be expressed by Equation (10). Moreover, the flows through the suction and discharge ports are modelled as an isentropic flow through an orifice as expressed in Equation (11), in which C_d and $A_{orifice}$ are the discharge coefficient and the orifice area, respectively (Subiantoro *et al.*, 2013).

$$m_{cv}\frac{du_{cv}}{dt} + u_{cv}\frac{dm_{cv}}{dt} = -\frac{d(PV)_{cv}}{dt} + \sum_i\left(h_i + \frac{v_i^2}{2}\right)\frac{dm_i}{dt} - \sum_e\left(h_e + \frac{v_e^2}{2}\right)\frac{dm_e}{dt} \tag{10}$$

$$\frac{dm}{dt} = \rho_i C_d A_{orifice}\sqrt{2\left(h_i - h_i^s\right)} \tag{11}$$

Using the rotational equivalent of the linear forces exerted on the cylinder and rotor bodies, as shown in Figure 3, the total power produced by the expander is calculated by Equation (12), where I and α stand for inertia and angular acceleration, respectively. It is assumed a constant rotational speed for the rotor shaft and hence the angular acceleration of the rotor can be neglected. The torque terms in this equation are the external torques exerting on the cylinder or rotor due to friction or leakage that is eliminated in this investigation.

$$P = \omega_r\left\{\begin{array}{l} F_{v,p}\left(r_r + \dfrac{l_{ve}}{2}\right) - I_r\alpha_r - I_c\alpha_c\left(\dfrac{r_r + l_{ve}}{r_c\cos\gamma}\right) + \left(\dfrac{r_r + l_{ve}}{r_c\cos\gamma}\right)\sum T_c + \sum T_r \\ -\dfrac{F_{v,n}}{|F_{v,n}|}\dfrac{dl_{ve}/dt}{|dl_{ve}/dt|}F_{v,f}\left(\left(r_c\sin\gamma - \dfrac{F_{v,n}}{|F_{v,n}|}\dfrac{W_v}{2}\right)\left(\dfrac{r_r + l_{ve}}{r_c\cos\gamma}\right) + \dfrac{W_v}{2}\right) \end{array}\right\} \tag{12}$$

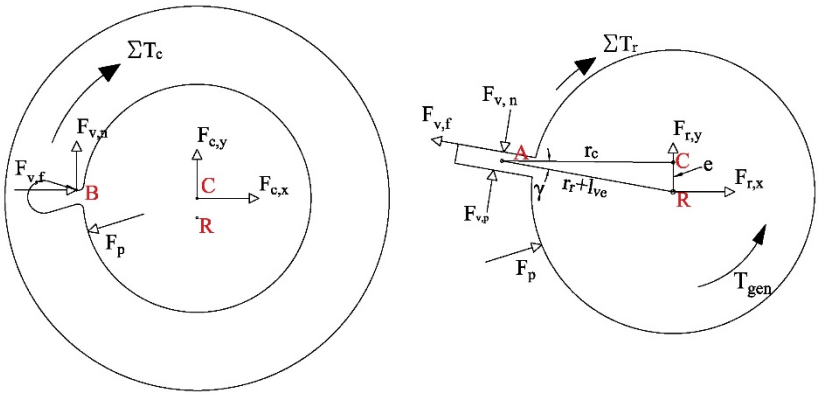

Figure 3: Free body diagram of the expander rotor and cylinder.

In Equation (12), friction and normal forces ($F_{v,f}$, $F_{v,n}$) exerted on the vane and forces, due to the pressure difference across the vane ($F_{v,p}$), are calculated using Equations (13) to (15), where η_v stands for the vane friction coefficient which is assumed to be 0.15. Moreover, the cylinder angular acceleration can be obtained from Equation (16) (Subiantoro, 2012).

$$F_{v,n} = \left(I_c \alpha_c - \sum T_c\right) \Big/ r_c \cos\gamma - \frac{dl_{ve}/dt}{\left|dl_{ve}/dt\right|} \eta_v \left(r_c \sin\gamma - \frac{W_v}{2}\right) \tag{13}$$

$$F_{v,f} = \eta_v \left|F_{v,n}\right| \tag{14}$$

$$F_{v,p} = \left(P_{scv} - P_{dcv}\right) l_{ve} l_{\exp} \tag{15}$$

$$\alpha_c = \alpha_r \left[\frac{2\left(r_r + l_{ve}\right)^2}{r_c^{\,2} + \left(r_r + l_{ve}\right)^2 - e^2}\right] + \omega_r \frac{dl_{ve}}{dt} \left[\frac{4\left(r_r + l_{ve}\right)\left(r_c^{\,2} - e^2\right)}{r_c^{\,2} + \left(r_r + l_{ve}\right)^2 - e^2}\right] \tag{16}$$

3. RESULTS

Based on the assumptions made in the methodology section and the operational and dimensional conditions shown in Table 1, the thermodynamic properties for the system at each node in Figure 2(A) are calculated assuming an isentropic pump. The lowest pressure for the system is 6 bar, which is within the pressure range acceptable for condensers (Drescher and Brüggemann, 2007). The net power output and mass flow rate are presented in Table 2. Since the expander dimensions dictate the mass flow rate of the system, R1234yf as a denser fluid gives a higher mass flow rate. Consequently, for an isentropic pump working under the same conditions, R1234yf and R1234ze(E) consumed almost 26% and 16% more power compared to R134a. The expander power generations with R1234yf and R1234ze(E) were almost equal. Although the internal effectiveness for the expander was almost 1% less for R1234yf compared to R1234ze(E), the cycle efficiency was slightly higher. It was also observed that the system was less efficient for both replacement fluids compared to R134a, but not significantly. Therefore, assuming the environmental characteristics of these fluids, R1234yf is a desirable choice within the operational condition in this study.

Table 2: Cycle performance parameters.

Working fluid	Mass flow rate (g/s)	Expander power output (W)	Pump consumed power (W)	Expander internal effectiveness (ε_{exp}%)	Cycle efficiency (%)
R1234yf	44.2	190	24	34.60	2.30
R1234ze(E)	42.3	191	22	34.67	2.27
R134a	39.8	194	19	34.90	2.29

As for the expander characteristics, Figure 4(A) shows the torque output for the expander versus rotation angle as well as inertia and pressure components of the torque output based on Equation (12) for R1234yf. It is obvious that the torque output for the expander was more dependent on the inertia component since the total torque almost followed the inertia term trend. The inertia component that is the product of cylinder angular acceleration and the inertia has an average of zero, while the pressure component that is due to pressure difference across the working chambers is non-zero. Hence, the average torque output for the R1234yf, R1234ze(E), and R134a were 1.80 *N.m*, 1.82 *N.m*, and 1.83 *N.m*, respectively. It is worth mentioning that the behaviors of the torque output for all three fluid are similar. Furthermore, Figure 4(B) compares the pressure inside the working chambers at one complete revolution of the expander. The pressure rose sharply at the very first angles due to suction volume chamber filling. Over this suction process, the pressure difference across the chambers is one of the parameters leading to system rotation. The suction process carried on up to the suction valve closure-

angle, which is the start of the expansion process. At the end of expansion, the discharge chamber received the expanded fluid and discharged it to the condenser. Figures for R1234ze(E) and R134a are very similar as that for R1234yf and as such are not shown in this paper. The lower-than-expected suction pressure observed at the final angles of rotation was due to the overexpansion in the system. To address this issue, the suction valve can be closed at an earlier angle compared to the closure-angle calculated using isentropic expansion.

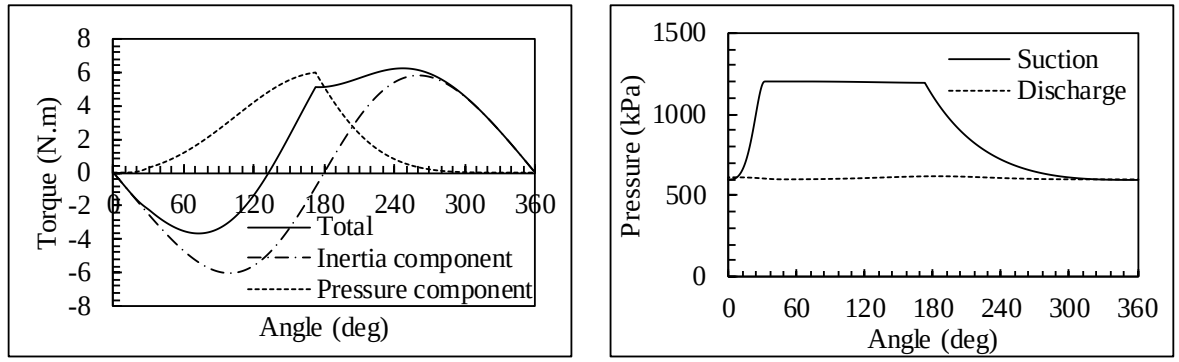

(A) (B)

Figure 4: (A) Torque outputs, and (B) Discharge and suction chambers pressures of the RV expander with R1234yf.

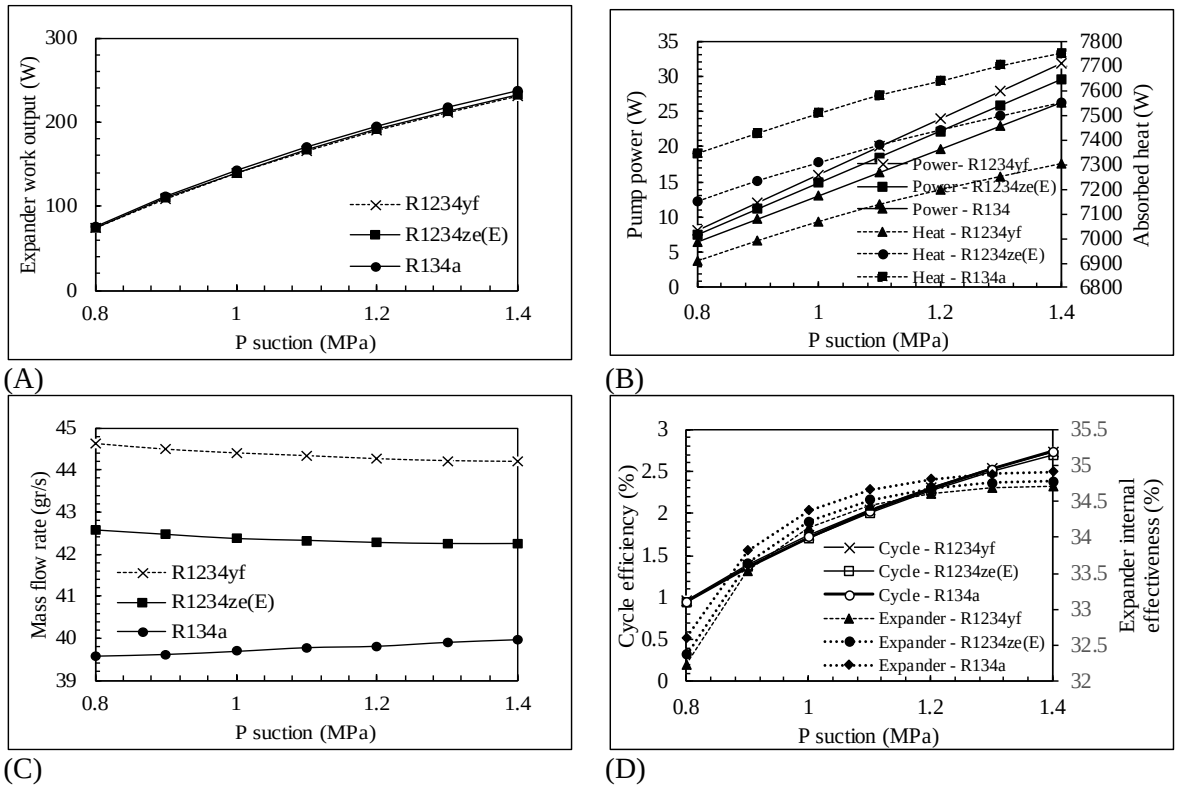

(A) (B) (C) (D)

Figure 5: (A) Expander power output (B) Pump power and absorbed heat, (C) Mass flow rate, and (D) Efficiencies for the cycle and expander, versus the variation of highest pressure of the cycle.

Figure 5(A) compares the expander power output versus suction pressure for R134a, R1234yf, and R1234ze(E). The expander power generation is as a function of inertia and pressure components based on Equation (12). The inertia term is the product between the cylinder inertia with the negative of the angular acceleration of the cylinder, whose average is zero (Subiantoro, 2012). Hence, the pressure component is the one that dictates the average torque output. An increasing suction pressure led to a

higher pressure difference across the vane and hence, the power output increased. Figure 5(B) illustrates the absorbed heat in the evaporator and the pump power consumption. The higher working pressure increases the enthalpy difference across the heat absorption process. Although the rate of this growth was decreasing, the heat absorption demonstrated insignificant change with respect to the mass flow rate alteration, which reached a minimum at 1.4 MPa for R1234yf, as shown in Figure 5(C). This also holds true for the pump power consumption. Figure 5(D) compares the efficiency of the cycle and the expander internal effectiveness versus suction pressure for R134a, R1234yf, and R1234ze(E). From the fluid viewpoint, both parameters are in decreasing order of R134a, R1234ze(E), and R1234yf. The cycle efficiency and the expander internal effectiveness grew gradually by increasing maximum working pressure, while the expander internal effectiveness increased slightly at higher suction pressures. It should be noted that these two replacement working fluids are chosen due to their promising environmental features, although these seem not to be as desirable as R134a for ORCs apart from their minimal environmental impact. Figure 6 compares the produced power at various suction pressures and rotational speeds ranged between 100 to 1000 rpm. To understand the trends, it is useful to remember that the torque is not only a function of pressure, but also of inertia. The higher rotational speed leads to a higher vane normal force due to the higher inertial component and consequently a higher frictional force, as shown in Equations (13) and (14). Therefore, there should exist an optimum point for the power output concerning the various suction pressures, although within this range of the operating speed, which is based on the actual working conditions of our RV expander prototype, no optimum value can be observed as it seems to lie beyond the range.

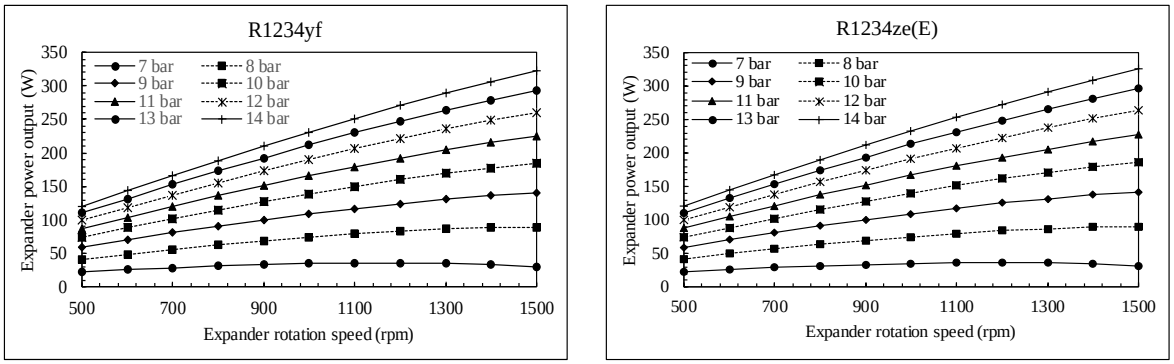

Figure 6: Power production versus different pressure and speeds.

4. CONCLUSIONS

In this study, the first law of thermodynamics is used to evaluate the performance of a Revolving Vane expander within an ORC system using R134a, R1234yf and R1234ze(E). Both R1234yf and R1234ze(E) have negligible Ozone Depletion Potential (ODP) and Global Warming Potential (GWP), but have similar thermodynamic properties as R134a. A basic Organic Rankine Cycle without any superheating and sub-cooling was assumed in this study, and cycle was analyzed by applying the conservation of mass and energy to each component within the cycle. This is to study the performance of the expander in the provided operating conditions. The RV expander was modelled using the specified operational and dimensional conditions, and comprised dynamics, thermodynamics and dynamics models. Assuming 12 and 6 bar as the highest and lowest pressures, and 1000 rpm as the expander operating speed, the expander produced almost same using R1234yf and R1234ze(E). Although the internal effectiveness for the expander was slightly less for R1234yf compared to R1234ze(E), the cycle efficiency was higher. The system was insignificantly less efficient with both replacement fluids compared to R134a. Therefore, assuming the environmental characteristics of these fluids, R1234yf is a desirable choice within the operational condition in this study. The performance analysis demonstrated that from the fluid viewpoint, both cycle efficiency and expander internal effectiveness are in decreasing order of R134a, R1234ze(E), and R1234yf. They grew gradually by increasing maximum working pressure, while the expander internal effectiveness almost plateaued at suction pressures higher than 1.2 MPa. An analysis on the expander rotational speed also showed that

there exists an optimum point for the power output concerning the various suction pressures, and the ORC efficiency decreased as the rotational speed increased. This study demonstrated the potential of an RV expander in an ORC system and this requires further investigation by including the inefficiencies effect of the system performance. These simulations results will be validated with the experimental data and will be reported in future publications.

NOMENCLATURE

C_d	Discharge coefficient	
e	Eccentricity	(mm)
F	Force	(N)
h	Enthalpy	(kJ/kg)
I	Inertia	($kg.mm^2$)
$l_{expander}$	Expander length	(mm)
$\dot{m}$	Mass flow rate	(kg/s)
P	Power; Pressure	(kW); (Pa)
Q	Heat transfer rate	(kW)
r	Radius	(mm)
T	Torque	(N.m)
T	Time	(s)
u	Internal energy	(kJ/kg)
V	Volume	(cm^3)
v	Speed	(m/s)
W	Work; Vane width	(kW); (mm)
Greek		
φ	Angle	(rad)
ω	Operation speed	(rad/s)
α	Angular acceleration	(rad/s^2)
ρ	Density	(kg/m^3)
ε	Internal isentropic effectiveness	(%)
γ	Angle in triangle ACR-Figure 3	(rad)
η	Friction coefficient	
Superscript		
a	Actual	
is	Isentropic	
Subscript		
r	Rotor	
c	Cylinder	
cv	Control Volume	
i	Inlet	
e	Eject/Outlet	

REFERENCES

Badr, O., O'Callaghan, P. W., Hussein, M., Probert, S. D., 1984, Multi-vane expanders as prime movers for low-grade energy organic Rankine-cycle engines, *Applied Energy*, 16: 129-46.

Bao, Junjiang, Zhao, Li, 2013, A review of working fluid and expander selections for organic Rankine cycle, *Renewable and Sustainable Energy Reviews*, 24: 325-42.

Dai, Yiping, Wang, Jiangfeng, Gao, Lin, 2009, Parametric optimization and comparative study of organic Rankine cycle (ORC) for low grade waste heat recovery, *Energy Conversion and Management*, 50: 576-82.

Drescher, Ulli, Brüggemann, Dieter, 2007, Fluid selection for the Organic Rankine Cycle (ORC) in biomass power and heat plants, *Applied Thermal Engineering*, 27: 223-28.

Giuffrida, Antonio, 2018, A theoretical study on the performance of a scroll expander in an organic Rankine cycle with hydrofluoroolefins (HFOs) in place of R245fa, *Energy*, 161: 1172-80.

Imran, Muhammad, Usman, Muhammad, Park, Byung-Sik, Lee, Dong-Hyun, 2016, Volumetric expanders for low grade heat and waste heat recovery applications, *Renewable and Sustainable Energy Reviews*, 57: 1090-109.

Lemort, V., Legros, A., 2017, 12 - Positive displacement expanders for Organic Rankine Cycle systems, *In:* Macchi, Ennio Astolfi, Marco (eds.), *Organic Rankine Cycle (ORC) Power Systems*, Woodhead Publishing: 361-96.

Lemort, Vincent, Quoilin, Sylvain, Cuevas, Cristian, Lebrun, Jean, 2009, Testing and modeling a scroll expander integrated into an Organic Rankine Cycle, *Applied Thermal Engineering*, 29: 3094-102.

Molés, Francisco, Navarro-Esbrí, Joaquín, Peris, Bernardo, Mota-Babiloni, Adrián, Mateu-Royo, Carlos, 2017, R1234yf and R1234ze as alternatives to R134a in Organic Rankine Cycles for low temperature heat sources, *Energy Procedia*, 142: 1192-98.

Ooi, Kim Tiow, Teh, Yong Liang, 2012, Revolving vane compressor, In.: Google Patents.

Subiantoro, A., 2012, Development of a revolving vane expander , Doctoral dissertation, Nanyang Technological University, Singapore.

Subiantoro, Alison, Ooi, Kim Tiow, 2014, Comparison and performance analysis of the novel revolving vane expander design variants in low and medium pressure applications, *Energy*, 78: 747-57.

Subiantoro, Alison, Tiow, Ooi Kim, 2009, Introduction of the Revolving Vane Expander, *HVAC&R Research*, 15: 801-16.

Subiantoro, Alison, Yap, Ken Shaun, Ooi, Kim Tiow, 2013, Experimental investigations of the revolving vane (RV-I) expander, *Applied Thermal Engineering*, 50: 393-400.

Yamada, Noboru, Mohamad, Md Nor Anuar, Kien, Trinh Trung, 2012, Study on thermal efficiency of low- to medium-temperature organic Rankine cycles using HFO−1234yf, *Renewable Energy*, 41: 368-75.